

# Direct observation of DNA overwinding by reverse gyrase

Taisaku Ogawa<sup>a</sup>, Katsunori Yogo<sup>a,1</sup>, Shou Furuike<sup>a,2</sup>, Kazuo Sutoh<sup>a</sup>, Akihiko Kikuchi<sup>b</sup>, and Kazuhiko Kinoshita Jr.<sup>a,3</sup>

<sup>a</sup>Department of Physics, Faculty of Science and Engineering, Waseda University, Shinjuku-ku, Tokyo 169-8555, Japan; and <sup>b</sup>Division of Molecular Mycology and Medicine, Nagoya University Graduate School of Medicine, Nagoya 466-8550, Japan

Edited by James M. Berger, Johns Hopkins University School of Medicine, Baltimore, MD, and approved April 27, 2015 (received for review November 20, 2014)

Reverse gyrase, found in hyperthermophiles, is the only enzyme known to overwind (introduce positive supercoils into) DNA. The ATP-dependent activity, detected at >70 °C, has so far been studied solely by gel electrophoresis; thus, the reaction dynamics remain obscure. Here, we image the overwinding reaction at 71 °C under a microscope, using DNA containing consecutive 30 mismatched base pairs that serve as a well-defined substrate site. A single reverse gyrase molecule processively winds the DNA for >100 turns. Bound enzyme shows moderate temperature dependence, retaining significant activity down to 50 °C. The unloaded reaction rate at 71 °C exceeds five turns per second, which is >10<sup>2</sup>-fold higher than hitherto indicated but lower than the measured ATPase rate of 20 s<sup>-1</sup>, indicating loose coupling. The overwinding reaction sharply slows down as the torsional stress accumulates in DNA and ceases at stress of mere ~5 pN·nm, where one more turn would cost only sixfold the thermal energy. The enzyme would thus keep DNA in a slightly overwound state to protect, but not overprotect, the genome of hyperthermophiles against thermal melting. Overwinding activity is also highly sensitive to DNA tension, with an effective interaction length exceeding the size of reverse gyrase, implying requirement for slack DNA. All results point to the mechanism where strand passage relying on thermal motions, as in topoisomerase IA, is actively but loosely biased toward overwinding.

reverse gyrase | topoisomerase | magnetic tweezers | DNA overwinding | torsion

Reverse gyrase, discovered in 1984 in a hyperthermophilic archaeon *Sulfolobus* (1) which was later classified as *Sulfolobus tokodaii* (2), is a unique DNA topoisomerase that can introduce positive supercoils into DNA (3–7). The only other enzyme that has the gyration activity is DNA gyrase, which introduces negative supercoils. Although DNA gyrase belongs to type II topoisomerase, which changes the linking number (Lk) of dsDNA by two by cutting and religating both strands simultaneously, reverse gyrase is of type IA topoisomerase (topo IA), where one strand is cut to allow the passage of the other, resulting in the Lk changes in steps of one (3–7). Reverse gyrase is found in hyperthermophilic archaea and eubacteria, and the positive supercoiling activity requires a temperature above 70 °C (8, 9). The enzyme is a 130-kDa single polypeptide, a fusion complex of two domains (10): The carboxyl terminal half is related to topo IA, whereas the amino terminal half has an ATP-binding site and is akin to helicase, although neither the whole enzyme nor the isolated helicase-like domain shows genuine helicase activity (11). A crystal structure of the full-length reverse gyrase (12) and more recent structures with additional features (13) all support the basic two-domain construct. The physiological roles of reverse gyrase are not yet fully clear, although positive supercoiling is expected to protect DNA from denaturation at the growth temperatures of hyperthermophiles.

Reactions of reverse gyrase have so far been analyzed in bulk assays on circular (plasmid) DNA. Basically, the enzyme only increases the Lk of DNA: relaxation of negatively supercoiled DNA, which does not require ATP and is rapid, and an ATP-dependent slower introduction of positive supercoils (14, 15). Single-stranded (ss) regions in DNA are required for binding and

positive supercoiling (16, 17). The supercoiling activity depends on the enzyme-to-DNA ratio, requiring a molar ratio of more than 10 for effective activity (15). However, when an ss bubble (continuous base pair mismatches) or an AT-rich sequence more than 20 bp long was inserted in a DNA substrate, the positive supercoiling activity became detectable at substoichiometric ratios (17). Positive supercoiling requires ATP, but the coupling appears loose in that many ATP molecules are hydrolyzed per introduced turn (18).

The mechanism of positive supercoiling has been discussed on the basis of the two distinct topo IA and helicase-like domains and a “latch” in between that appears to lock the topo IA domain in a closed conformation (12). Strand passage likely takes place in the topo IA domain, and the passage must somehow be biased toward overwinding with the energy supplied by ATP hydrolysis. The helicase-like domain alters its affinity for dsDNA and ssDNA depending on the bound nucleotide (7), hinting at how ATP hydrolysis is coupled. However, crucial information, such as the processivity, individual kinetics, and overwinding torque, is still scarce. The activity inferred from bulk studies is quite low (17, 18), at most on the order of one superhelical turn per minute, which might be limited by the assay methods.

Motivated by recent single-molecule studies that have revealed the operation of various topoisomerases in real time (19–23), we have observed the activity of purified reverse gyrase from *S. tokodaii* (4) under an optical microscope at 71 °C (Fig. 1). A magnetic bead was tethered to a glass surface with linear dsDNA. When reverse gyrase overwound the DNA, the bead rotated, or sank when rotation was constrained. Inclusion of an ss bubble in

## Significance

Reverse gyrase resides in bacteria that live in hot conditions. The enzyme further intertwines the double helix of DNA to make it tighter. In biochemical assays, reverse gyrase appears quite inefficient, requiring many enzyme molecules per DNA and yet taking many minutes to wind it up. Here, we show that one reverse gyrase molecule rapidly overwinds relaxed DNA but begins to idle as torsion accumulates. Excess torsion would hamper replication/transcription activities, whereas quick restoration of modest torsion prevents thermal denaturation of DNA. We discuss how reverse gyrase lets one strand of DNA pass the other in a preferred direction to achieve overwinding.

Author contributions: T.O. and K.K. designed research; T.O. performed research; K.Y., S.F., and K.S. contributed new reagents/analytic tools; A.K. prepared reverse gyrase; T.O. analyzed data; and T.O., A.K., and K.K. wrote the paper.

The authors declare no conflict of interest.

This article is a PNAS Direct Submission.

Freely available online through the PNAS open access option.

<sup>1</sup>Present address: Graduate School of Medical Sciences, Kitasato University, Sagamihara, Kanagawa 252-0373, Japan.

<sup>2</sup>Present address: Department of Physics, Osaka Medical College, Takatsuki 569-8686, Japan.

<sup>3</sup>To whom correspondence should be addressed. Email: kazuhiko@waseda.jp.

This article contains supporting information online at [www.pnas.org/lookup/suppl/doi:10.1073/pnas.1422203112/-DCSupplemental](http://www.pnas.org/lookup/suppl/doi:10.1073/pnas.1422203112/-DCSupplemental).

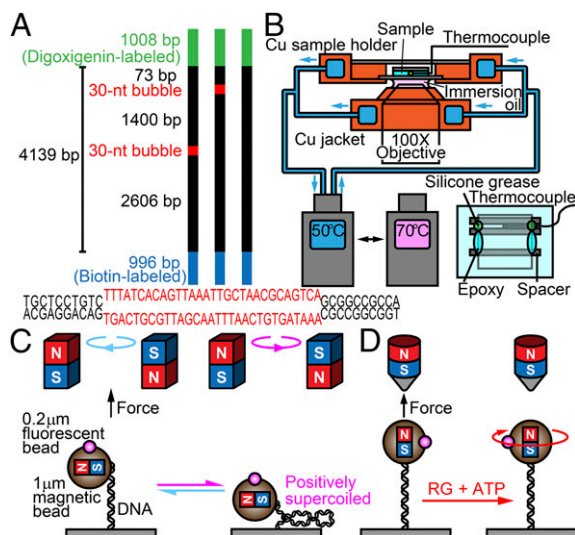


**Fig. 1.** Experimental design. (A) DNA constructs. (Bottom) Bubble sequence is shown. (B) Temperature control. (Bottom Right) Top view of a sample chamber. (C) Selection of DNA under a magnet pair. The bead, with a preferred axis for magnetization, must be on the side of the DNA, and the bead must sink when it is rotated in the overwinding direction. N, North; S, South. (D) Observation of DNA overwinding reaction by reverse gyrase under a single magnet, which allows free rotation of the bead. The bead rotates to relax the torsional stress in DNA introduced by reverse gyrase (RG).

the DNA greatly enhanced the activity, which we analyze to infer the underlying mechanism.

## Results

**Real-Time Observation of DNA Overwinding Activity.** We prepared three kinds of linear DNA substrates, two with a bubble 30 nt long at different (middle and end) positions and one without a bubble (Fig. 1A; details in Fig. S1). One end of the DNA was attached to the coverslip surface through biotin-streptavidin linkages, and the other end was attached to a 1-μm magnetic bead through digoxigenin/antidigoxigenin antibody linkages. Small fluorescent beads were attached to the magnetic bead to facilitate observation of rotation. After infusing reverse gyrase in a medium containing 5 mM ATP and 10 mM MgCl<sub>2</sub>, the sample was set on an inverted microscope and the temperature was controlled to within ±1 °C as monitored with a thermocouple placed next to the sample (Fig. 1B).

We started an assay by searching at 50 °C for a bead to be analyzed that satisfied the following conditions:

- i) The number of fluorescent daughter beads had to be one or two for unambiguous tracing of rotation.
- ii) The magnetic bead had to be tethered by one unnicked DNA molecule. For this selection, we used a horizontal pair of magnets to pull the bead upward at 0.5–0.9 pN and rotated the bead for 30 turns in the overwinding (counterclockwise as viewed from above) direction. This operation should lower the bead (Fig. 1C); otherwise, the DNA is nicked. Rotation in the opposite (unwinding) direction, in contrast, should not lower the bead appreciably at this relatively high tension (24), unless the bead is tethered by two or more DNA molecules. The latter unwinding test, however, was postponed until all measurements in an observation chamber were finished, because unwinding might lead to excess binding of reverse gyrase. In fact, we never encountered the case of multiple tethering because the surface density of DNA was low, such that only several beads were observed in the field of view measuring 49 × 65 μm<sup>2</sup>.
- iii) The magnetic bead must be on a side of DNA in the horizontal field in test ii (Fig. 1C), because we were to apply a

vertical magnetic field for the reverse gyrase assay (Fig. 1D). Thus, we selected a bead of which the center itself rotated along a large circular orbit, deselecting those beads that rotated only on their own axis. After the rotation test, we wound back the bead for 30 turns to relax the DNA. On average, one bead in ~10 fields of view passed the three tests.

Once a candidate bead was found, we replaced the horizontal magnets with a vertical magnet (Fig. 1D) to pull the bead upward at 0.5 pN while allowing free rotation. After confirming the bead to rotate (or to undergo rotational diffusion) nearly on its own axis, we turned on fluorescence excitation and started the observation for analysis for 5 min at 50(±1) °C, followed by another 5 min at a higher temperature and 5 min at 50 °C again. At the end, we repeated test ii above. About 10% was found to be nicked by this time, and we discarded such data. We then searched for another bead in the same chamber, starting with test i above. Typically, one chamber was on the heating stage for 2–3 h, and not for more than 3 h, during which time three to 10 beads were recorded for detailed analysis.

**Overwinding Activity Leads to Indefinite Rotations.** At 71 °C and with 10 nM reverse gyrase, beads tethered by the three different DNA substrates all rotated clockwise when viewed from above (Fig. 2). This direction is as expected for overwinding of the right-handed DNA double helix by reverse gyrase, because the bead at the free end should rotate to relax the overwound state. At 10 nM enzyme, the rotation continued indefinitely: We never observed a conspicuous long (>100 s) pause except for complete cessation of rotation due to DNA nicking. Such an unlimited rotation is not possible with circular DNA (unless nicked).

The significant overwinding of the nonbubble DNA is accounted for by the presence of AT-rich sequences in the substrate (AT content per 20 bp reaches 80% or 85% in eight stretches each sized 20–35 bp). With the bubble, the rotation was much faster at 71 °C: 0.23 ± 0.03 revolutions per second (rps) (mean ± SD for *n* = 8 beads; all errors in this paper are SDs) for mid-bubble and 0.27 ± 0.07 rps for end bubble (*n* = 11), compared with 0.079 ± 0.028 rps for nonbubble DNA (*n* = 9). Bulk observation (17) has also shown that a bubble greatly promotes the reverse

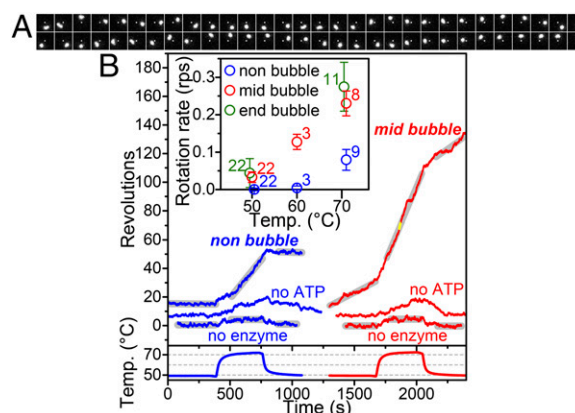


**Fig. 2.** Overwinding of DNA by reverse gyrase leads to indefinite rotations. (A) Sequential images at 132-ms intervals of a fluorescent daughter bead attached to a tethered magnetic bead. White dots show the center of rotation. View from above in Fig. 1D. The image size is 2.8 × 2.8 μm<sup>2</sup>. The images are from the yellow portion of the red curve in B. Also see Movie S1. (B) Time courses of bead rotation at 10 nM reverse gyrase and monitored sample temperature. Thick straight lines show the linear fit to the portion within ±1 °C of 50 °C or 71 °C, from which the average rotary speed is calculated. (Inset) Temperature dependence of the average rotary speeds at 10 nM reverse gyrase under DNA tension of 0.5 pN. Numbers are *n* (beads examined; approximately twice the number of beads for 50 °C, where the second measurement occasionally failed), and error bars show SD.



gyrase activity. Our results, in addition, demonstrate that reverse gyrase can overwind DNA even at 50 °C, albeit slowly, where bulk activity has not been reported. The temperature dependence for bubbled substrates (Fig. 2*B*, *Inset*) is moderate and gradual, and it is independent of the position of the bubble. In contrast, we did not observe unidirectional rotation with the nonbubble DNA at 60 °C or below. Thermal melting is negligible at 60 °C, and an ss region needed for reverse gyrase binding is virtually absent. Even at 71 °C, ss regions created by thermal melting should be transient and unstable, and the separated strands may not be long enough for efficient strand passage. A stable bubble would thus warrant a faster reaction.

We show below that the activity of reverse gyrase is highly sensitive to the tension and torsional stress in DNA. The results shown in Figs. 2 and 3 were all under 0.5 pN of tension. Torsional stress is determined by the viscous friction against the rotating bead and is given by  $\pi D^3 \eta \omega$ , where  $D$  is the bead diameter,  $\eta$  is the viscosity of water, and  $\omega$  is the bead rotation speed in radians per second. For the mid-bubble DNA, the stress was 1.8 pN·nm at 71 °C (0.36 pN·nm at 50 °C), and for the nonbubble DNA, it was 0.62 pN·nm at 71 °C. Reverse gyrase worked against this much counteracting torque.

In the absence of the enzyme, we observed only Brownian rotations of the bead, with rms excursions of  $290 \pm 50^\circ$  (5 min each for six beads) at 71 °C and  $290 \pm 40^\circ$  at 50 °C ( $n = 10$ ) for the nonbubble DNA. These values for the DNA contour length of  $\sim 1.4 \mu\text{m}$  imply a torsional persistence length of 55 nm and are commensurate with the torsional elasticity of B-form DNA (25). We also note that heating from 50 to 71 °C in the absence of

reverse gyrase resulted in a clockwise rotation of  $3.5 \pm 0.7$  revolutions ( $n = 6$ ) as seen at the bottom of Fig. 2*B*. This finding is consistent with the reported unwinding rate of  $-0.0105^\circ\text{C}^{-1}\text{bp}^{-1}$  covering this temperature range (26). The presence of a bubble changed these values only slightly (analyzed for the mid-bubble): Fluctuations were  $410 \pm 40^\circ$  ( $n = 4$ ) at 71 °C and  $290 \pm 50^\circ$  ( $n = 7$ ) at 50 °C, and the thermal unwinding from 50 to 71 °C was  $4.5 \pm 1.2$  revolutions ( $n = 4$ ). The effects of the bubble on the physical properties of DNA appear localized.

Without ATP, reverse gyrase gradually unwound DNA at 71 °C, and the unwinding was slowly reversed upon cooling (Fig. 2*B*, *Middle*; longer records are shown in Fig. S2). Presumably, reverse gyrase binds to where DNA happens to melt, with such occurring in succession because bead rotation keeps the DNA relaxed. In the presence of ATP, in contrast, reverse gyrase continually overwinds DNA, hindering melting and preventing excess binding of reverse gyrase. Indeed, we observed little reverse rotation upon cooling to 50 °C (Fig. 2*B*, *Top* and Fig. S2). As expected, unwinding of circular plasmids in the absence of ATP requires nicking (27).

**Reverse Gyrase Works Processively.** To gain insight into the mechanism of strand passage, we focus below on the mid-bubble substrate. The ss region needed for binding and strand passage is well defined and preserved in the bubble, compared with thermally induced binding sites where base pairs are broken and reformed dynamically. The end bubble gave indistinguishable behaviors, but we avoid possible complication due to the nearby bead.

To see whether the observed continuous rotation was effected by successive operations of many reverse gyrase molecules, we decreased the enzyme concentration into the picomolar range (Fig. 3). Both at 50 °C and 71 °C, we did not notice an appreciable difference in rotation behaviors until we went down to 0.1 nM, below which finding a rotating bead became difficult. Those beads that did rotate, however, rotated at speeds indistinguishable from the speed at 10 nM. The implication is that one reverse gyrase stays on the bubble for hundreds of seconds [dissociation rate ( $k_{\text{off}}$ )  $< 10^{-2} \text{ s}^{-1}$ ], introducing many positive turns ( $> 100$  on average at least at 71 °C) processively. The average speed was  $0.24 \pm 0.07$  rps ( $n = 20$  for all reverse gyrase concentrations) at 71 °C and  $0.046 \pm 0.022$  rps ( $n = 39$ ) at 50 °C, which we interpret as the catalytic rate of the bound enzyme under DNA tension of 0.5 pN and counteracting torque of 1.9 pN·nm (71 °C) or 0.50 pN·nm (50 °C). The rate increases 5.2-fold per 21 °C, corresponding to the temperature coefficient  $Q_{10}$  of 2.2, which is within the range for usual enzymes. To some extent, the rotary rate varied from bead to bead (Fig. 3*A* and *B*) for an unknown reason; however, the concentration dependence argues against the possibility that faster rotations were driven by two or more enzyme molecules.

From Fig. 3*D*, we estimate the dissociation constant,  $K_{\text{d}}$ , of reverse gyrase for the bubble to be roughly 30 pM (between 10 and 100 pM) both at 50 °C and 71 °C. The high affinity is commensurate with the low  $k_{\text{off}}$  above. At 50 °C, some of the rotation time courses appear to be punctuated with pauses on the order of  $\sim 100$  s (shorter pauses may also exist at 71 °C), although Brownian fluctuations hamper clear distinction. If the pauses are real, reverse gyrase tends to work in a stop-and-go fashion at low temperatures while clinging to the bubble; the pauses are unlikely to represent dissociation and rebinding of the enzyme, because pausing patterns are similar at high- and low-enzyme concentrations and, at 10 pM in particular, rebinding within 100 s would imply too high a binding rate ( $k_{\text{on}}$ ) exceeding  $10^9 \text{ M}^{-1}\text{s}^{-1}$ .

**Plectoneme Formation by Reverse Gyrase.** In the experiments above, torsional stress remained low thanks to bead rotation. To see the effect of torsion, we used horizontal magnets to prevent bead rotation (Fig. 4*A*). Overwinding by reverse gyrase would then introduce plectonemes in the DNA, and the bead would sink toward the bottom, as was indeed observed. Formation of plectonemes

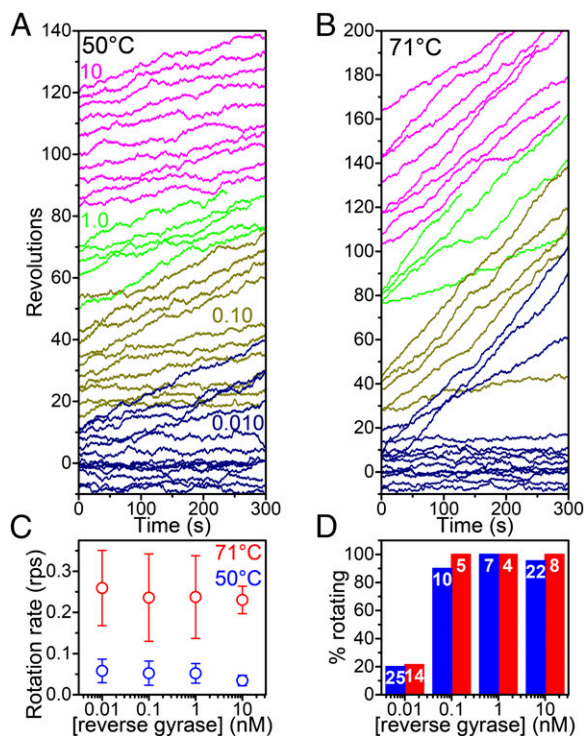


**Fig. 3.** Concentration dependence of overwinding activity at 0.5 pN of tension. (*A* and *B*) Rotation time courses at two temperatures. Colored numbers show [reverse gyrase] in nM. (*C* and *D*) [Reverse gyrase] dependence of the rotary speed (*C*) and the probability of rotation (*D*). Curves in *A* and *B*, with additional data to include all beads that satisfied conditions *i-iii* in the main text, are each fitted with a straight line to give individual rotary speeds, which are classified as rotating ( $> 0.01$  rps) or nonrotating ( $< 0.01$  rps). The average speed of rotating beads is shown in *C*, with error bars showing SD. Numbers in *D* show the total beads analyzed (71 °C) or approximately twice the number of beads (50 °C; data from 50-60-50 °C measurements are included).

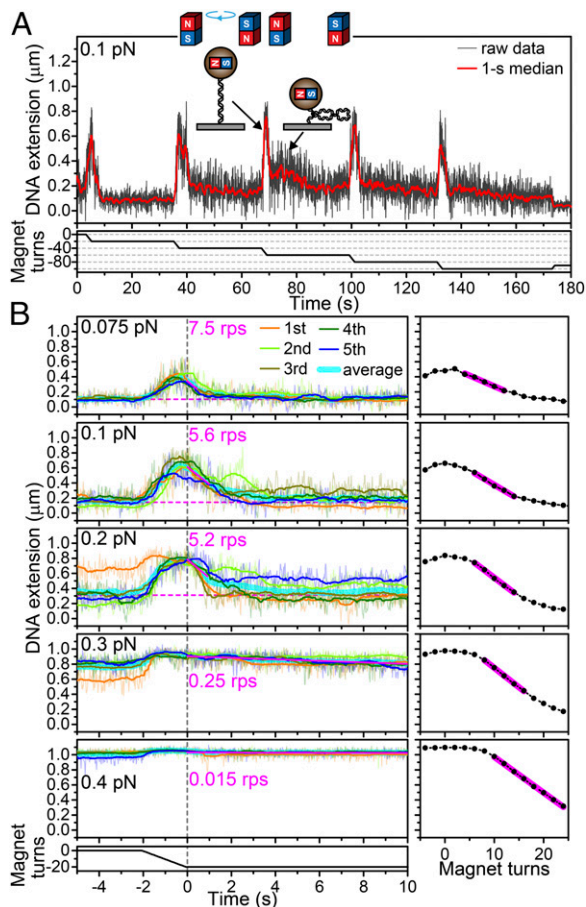


**Fig. 4.** Plectoneme formation by reverse gyrase. (A) Repetitive bead sinking in response to unwinding magnet rotation at 0.1 nM reverse gyrase. Unwinding magnet turns are taken as negative. After several trials under the same tension, we rotated the magnets in the overwinding direction to let the bead sink close to the surface (end of the curve). We then changed the tension and repeated the same procedure. (B, Left) Sinking time courses at various tensions for the bead in A. Individual time courses distinguished by colors are first 1-s median-filtered (smoother curves), aligned at the end of unwinding rotation (time 0), and averaged (thick cyan curve). At  $\leq 0.2$  pN, where sinking is significant, we fit the average with the magenta line between 0 s and the midpoint of sinking, with the final level (magenta dashed line) being estimated at 24–29 s; at  $\geq 0.3$  pN, the fit is between 0 and 10 s. Magenta numbers show estimated overwinding rates. (B, Right) Bead sinking by magnet rotation in the absence of reverse gyrase. Magenta lines show linear fit (also see Fig. S3).

requires a certain torque that depends on the tension on DNA; thus, we learn how much torque reverse gyrase can generate.

This supercoiling experiment was done at 71 °C, without the fluorescent daughter beads. We set the sample on the hot stage and waited for temperature equilibration, during which time the beads that would sink (tethered by unnicked DNA) already sank. We first rotated the magnets in the unwinding direction to raise the beads. We selected those beads that rotated around their own axis (i.e., those beads that were above the DNA) (Fig. 4A). We estimated the bead height (DNA extension) by deliberately defocusing the bead image and measuring the size of the diffraction ring (Fig. S3A). Because we observed the height rather than the orientation of the bead, fluctuations of the bead did not seriously hamper the analysis; thus, we were able to reduce DNA tension. In fact, we observed bead sinking only at tensions below  $\sim 0.3$  pN and none at 0.4 pN. After 30–60 s, we rotated the bead 20 turns at 10 rps in the unwinding direction, which brought the bead back to the original height. Unwinding by 30 turns did not

change results. Excess underwinding would be rapidly relaxed by reverse gyrase. In this way, we could repeatedly observe bead sinking for the same bead/DNA pair (Fig. 4A). Because individual sinking records varied considerably among successive trials, we averaged five to 10 successive runs under the same tension, taking the end of the unwinding maneuver as time 0 (thick cyan lines in Fig. 4B).

To convert the observed change in DNA extension into the number of overwinding turns introduced by reverse gyrase, we rotated the bead by magnets in small steps in the absence of reverse gyrase (Fig. 4B, Right and Fig. S3). The results at 71 °C are qualitatively similar to the results at room temperature (28). Starting from a relaxed DNA with  $m$ , the imposed number of turns, of zero, the extension  $z$  decreases with  $m$  initially slowly until a first plectoneme loop is formed. Thereafter,  $z$  decreases linearly as additional loops are introduced to keep the torsional stress in DNA constant. The decrease slows down again as  $z$  approaches zero, presumably because the DNA beneath serves as a cushion. We use the slope  $dz/dm$  in the linear portion (magenta lines in Fig. 4B, Right) to estimate the activity of reverse gyrase. In the sinking curves observed in the presence of reverse gyrase (Fig. 4B, Left), we would expect, after a small lag for the first several turns, a decrease of  $z$  at a constant rate. The initial lag, however, was not discerned because reverse gyrase works fast while the torsional stress is low (see below). We therefore took the initial slope,  $dz/dt$ , where  $t$  is time, of the average sinking curve (cyan lines in Fig. 4B, Left) as the sinking rate. Division by  $dz/dm$  gives  $dm/dt$ , the activity in revolutions per second during the plectoneme growth phase. The results at 0.1 nM and 1 nM reverse gyrase are summarized in Fig. 5A. The trend suggests that single reverse gyrase works at  $>5$  rps in the absence of tension and torsional stress. Comparison of Fig. 4B (Left vs. Right) indicates that reverse gyrase can introduce up to 10–20 positive supercoils in this DNA with  $Lk_0$ ,  $Lk$  at relaxed state, of  $\sim 400$ . The  $Lk$  density  $\sigma = \Delta Lk/Lk_0$  reaches  $+0.025 \sim +0.05$ , consistent with biochemical assays (see below).

**Dependence on Tension and Torsional Stress in DNA.** We varied tension to obtain Fig. 5A, but torque also varied simultaneously. The torque needed for plectoneme growth can be estimated from the DNA extension vs. rotation curves in Fig. 4B (Right). Mosconi et al. (28) have shown that their extension-rotation curves under various tension and salt conditions can all be approximated by one simple equation developed by Clauvelin et al. (29), which reads  $\Gamma = 2F(dz/dm)L_0/3\pi z_0$ , where  $\Gamma$  is the torque for plectoneme growth,  $F$  is the tension,  $dz/dm$  is the slope in the linear part,  $L_0$  is the contour length of DNA, and  $z_0$  is the extension at  $m = 0$ . We take  $L_0$  as 1,400 nm and estimate  $dz/dm$  and  $z_0$  from Fig. 4B (Right) and Fig. S3C to obtain  $\Gamma$ . In Fig. 5B, we replot Fig. 5A against  $\Gamma$ . We also include the free rotation result at  $F = 0.5$  pN and  $\Gamma = 1.9$  pN·nm (orange square in Fig. 5A and B). The two panels in Fig. 5A and B show the same data, where the effects of tension and torque are convolved. Below, we try to differentiate between the two effects.

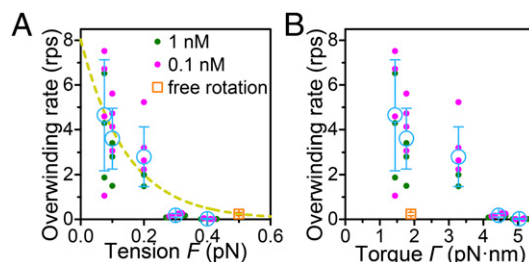


**Fig. 5.** Overwinding activity plotted against DNA tension  $F$  (A) and torque  $\Gamma$  required for plectoneme growth (B). Dots represent individual beads; circles represent their average, with error bars showing SD; and squares represent free rotation results from Fig. 3C. The dashed line in A shows the fit with  $\exp(-F\delta/k_B T)$ .



In Fig. 5A, the overwinding rate is zero at 0.4 pN, but tension cannot be the reason why because finite activity is observed at 0.5 pN (orange square in Fig. 5A). The decisive factor is torque (Fig. 5B): Reverse gyrase ceases to overwind DNA when opposed by a critical torque  $\Gamma_c$  of  $\sim 5$  pN-nm. Twisting DNA by one revolution against  $\Gamma_c$  would cost  $2\pi\Gamma_c \sim 30$  pN-nm of work, which is only sixfold the thermal energy and one-third to one-fourth of the free energy obtained by hydrolyzing one ATP molecule. This is the maximal work reverse gyrase can do in a productive catalytic cycle.

The activity sharply depends on torque only near  $\Gamma_c$ . In Fig. 5B, the activity drops more than an order of magnitude between 3.3 and 4.4 pN-nm, but the torque dependence is quite moderate below 3.3 pN-nm; note that tension must also contribute to the decrease in activity. Then, if we neglect in Fig. 5A the two points at 0.3 and 0.4 pN (4.4 and 5.0 pN-nm of torque), the other four points, including the orange one, would represent, roughly, the tension dependence alone. The four points can be fitted (dashed line in Fig. 5A) with an Arrhenius dependence,  $\exp(-F\delta/k_B T)$ , giving an interaction length  $\delta$  of  $\sim 32$  nm ( $k_B T = 4.7$  pN-nm for  $T = 344$  K). The two points at 0.1 and 0.5 pN, in particular, are nearly at the same torque of  $\sim 1.9$  pN-nm (Fig. 5B), suggesting that the fit indeed approximates tension dependence. Tension dependence is continuous, although strong with the large  $\delta$ , whereas torque impedes only near  $\Gamma_c$  and completely blocks net overwinding at  $\Gamma_c$ .

**Hydrolysis of ATP.** To see if overwinding activity is tightly coupled with ATP hydrolysis, we measured the rate of ATP hydrolysis in bulk solution (Fig. 6 and Fig. S4). At 71 °C, significant hydrolysis occurred without reverse gyrase. Reverse gyrase alone showed little hydrolysis activity, but DNA promoted hydrolysis. The hydrolysis activity with bubbled DNA was  $20$  s $^{-1}$ , more than twice the estimated overwinding activity at no load (Fig. 5A), indicating loose coupling as previously reported (18).

## Discussion

Microscopic imaging and manipulation at the high temperatures are far more difficult than at room temperature. Severe drifts limit precision. The sample must not contain heat-labile components, and, even then, the measurement is a race against thermal deterioration. We have partially solved these problems and shown that reverse gyrase works  $>10^2$  faster than hitherto indicated in bulk assays. In a bulk assay (17) with a 3.1-kbp bubbled plasmid ( $Lk_0$  of  $\sim 300$ ), the product with the highest  $\Delta Lk$  of  $\sim +10$  began to appear by 15 min but not at 7 min, when 4 nM reverse gyrase was mixed with 8 nM DNA at 80 °C, indicating an activity of  $\sim 10$  turns per 10 min per 0.5 enzyme/DNA, or  $\sim 0.03$  rps at 80 °C. Our direct

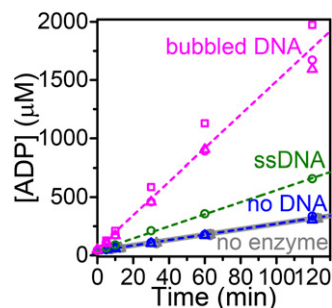


**Fig. 6.** DNA-dependent ATPase activity of reverse gyrase at 71 °C. Reverse gyrase (10 nM) was incubated with 5 mM ATP and 100 nM DNA (147-nt ssDNA or dsDNA containing a bubble). Each time course with a different symbol was fitted with a line to obtain an individual rate, although averaged lines are shown here. The hydrolysis rate without enzyme was  $2.3 \pm 0.1$   $\mu\text{M}\cdot\text{min}^{-1}$  ( $n = 3$ ). This value was subtracted from other rates to give the ATPase activity of reverse gyrase of  $20 \pm 3$  s $^{-1}$  with bubbled DNA ( $n = 3$ ),  $4.8$  s $^{-1}$  with ssDNA ( $n = 1$ ), and  $0.0 \pm 0.3$  s $^{-1}$  without DNA ( $n = 2$ ).

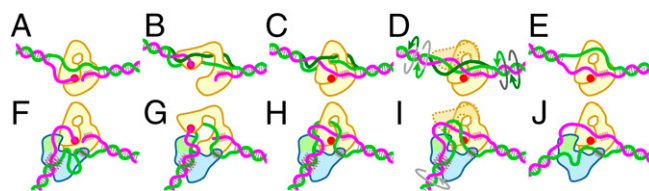


**Fig. 7.** Chiral operation by reverse gyrase. (A–E) Presumed mechanism of passive strand passage in topo IA. The magenta strand is held (hatched) in a groove. (A) Catalytic tyrosine (red circle) cuts the strand and binds one end. (B) Thermal opening of the gate to the central cavity allows thermal strand passage in either direction (light or dark green). (C) When the gate closes and the cut strand happens to be religated, the Lk has changed by one ( $\Delta Lk = \pm 1$ ). (D) Reopening of the gate without strand scission allows the green strand to exit from the cavity. The  $\Delta Lk$  localized in the ss region is spread (diluted) into the entire DNA through rotation of the ss/ds junction. (E) Enzyme is then ready for another passage. All events are stochastic and reversible. (F–J) In reverse gyrase, gate opening is likely controlled by ATP hydrolysis in the helicase domain (light blue) through the latch domain (light green). Biased strand passage may occur as follows. The ds/ss junction on the scissile side (F, Left) and a distant part of the green strand (F, Right) are both bound to the enzyme. (G) Coupled to unlocking of gate motion, the ds region elongates by base pairing, rotating the two ss ends to bias the passage correctly. Religation occurs while the bias is effective (H), and the green strand exits with  $\Delta Lk = +1$  (I). The gate is locked, and DNA is allowed to rotate to export the  $\Delta Lk$  (I→J). The export would fail if the DNA were already highly overwound. Many variations of this scheme are possible.

observation at 71 °C, in contrast, shows that the activity is at least  $\sim 5$  rps (Fig. 5A).

Reverse gyrase sharply slows down as  $\Gamma$  approaches  $\Gamma_c$  (Fig. 5B). In bulk assays with circular DNA,  $\Gamma$  increases as more supercoils are introduced. The bulk result above of  $\Delta Lk = 10$  implies an Lk density  $\sigma$  of  $\sim 0.03$ . For this  $\sigma$ , theory (30) predicts a torsional stress of  $\sim 5$  pN-nm at no tension (plasmids do not bear tension). This value agrees with our experimental  $\Gamma_c$ , explaining why the bulk activity near the end point was so low. There was a sign of a faster phase, but quantification is difficult in gel analyses. In any event, the kinetic features revealed here, quick overwinding at low torsional stress and sharp cessation at a moderate stress, aptly suit the physiological role of reverse gyrase if the demand is to keep DNA slightly overwound to protect, but not overprotect, the genome of hyperthermophiles against thermal denaturation and to restore the protected state quickly after thermal or replication/transcription-related perturbations.

The rather small  $\Gamma_c$  that limits the reverse gyrase activity is as expected if the strand passage mechanism in reverse gyrase is basically the same as the strand passage mechanism in genuine topo IA (5) (Fig. 7A–E). In topo IA, strand passage is a passive process relying on thermal fluctuations of the strand and the enzyme. The preference between the two modes of passage (light or dark green in Fig. 7C) is determined by the overall torsional stress in the DNA; thus, on average, the reaction tends to relax the DNA ( $Lk$  approaches  $Lk_0$ ). Reverse gyrase, in contrast, must increase Lk beyond  $Lk_0$  by actively biasing the direction of strand passage. In one proposal (5) for circular DNA, binding of reverse gyrase to DNA induces local DNA unwinding, whereas the rest of DNA is overwound. ATP then allows topoisomerase action on the unwound region to increase the Lk by 1. In this model, correct bias comes from the initial unwinding and the restoring pressure from the overwound region. In our bubbled linear DNA, however, the substrate site is unwound from the beginning and bead rotation cancels overwinding. Wrapping of DNA around reverse gyrase could also provide a bias (12), but whether it works with a bubble is not clear. Models starting with thermally melted DNA (7, 31) are readily compatible with our bubble results. Bias may originate from binding of the double-stranded (ds) or ss region in a specific manner (7) or by alternation of ss and ds bindings (31).

Here, we show a variant of the latter in Fig. 7 *F–J*, without compelling evidence. The bias comes from base pairing at the ds/ss junction, as would happen as a reversal of the duplex unwinding shown for the helicase domain (32). The pairing rotates the ends of the two single strands to bias strand passage correctly. During passage, all four ends of the two single strands are bound to the enzyme to isolate the ss region from the stress in the rest of DNA. After passage, however, the positive twist in the ss region must be exported to the entire DNA. This process is sensitive to the torsional stress in the entire DNA, and it fails when the opposing stress is too high. If the opposing stress exceeds  $\Gamma_c$ , the model predicts underwinding, which we indeed observed (Fig. S5). A priori, the enzyme could work against a high stress if the active bias might somehow accumulate over successive cycles. For the accumulation, all four ends must always be under control and continuously twisted as in a hand-over-hand fashion, a mechanism not readily conceivable in the known structures of reverse gyrase. Perhaps there is no physiological need for excessive overwinding, which would actually be harmful.

The mechanism above relying on stochastic thermal motions implies loose coupling with ATP hydrolysis, which we indeed observed. Unlocking of the gate by ATP hydrolysis does not necessarily accompany strand passage, and the passage may occasionally occur in the wrong direction. The wrong bias is the norm when exposed to torsional stress exceeding  $\Gamma_c$  (Fig. S5), implying that after reaching  $\Gamma_c$ , reverse gyrase would continue vain cycles either forward or backward with equal probability, consuming ATP.

The high tension dependence with the unusually large interaction length  $\delta$  of  $\sim 32$  nm, far exceeding the dimension of reverse gyrase of  $\sim 13$  nm (12), is also consistent with the above mechanism. A large value of  $\sim 10$  nm has also been reported for topo IA working on a bubbled DNA (20). Threading the green strand through the cavity (Fig. 7) would require an extra length compared with the magenta strand. Indeed, topo IA working on a bulged substrate, where one ss arm was much longer than the

other, was insensitive to tension (20). In reverse gyrase, in addition, all four ends of the two strands must be bound for biased passage while the two ss portions are sufficiently slack. Holding four ends likely requires overall bending of the DNA, as in Fig. 7. Tension thus impedes the operation of reverse gyrase.

## Methods

Reverse gyrase was purified from *S. tokodaii* as described (4). The bubbled DNA substrates shown in Fig. 1A were prepared as in Fig. S1, appending multiply biotinylated and digoxigenin-labeled ends. The biotinylated ends were attached to a coverslip modified with biotinylated polyethylene glycol. We attached to the other ends carboxylated superparamagnetic beads (1- $\mu$ m diameter) coated with antidigoxigenin antibody. For the rotation experiments in Figs. 2 and 3, we added fluorescent daughter beads (0.2- $\mu$ m diameter), which we found to bind to the magnetic beads. Assays were made in 50 mM Tris-HCl (pH 7.9 at 23 °C) containing 0.1 mM EDTA, 50 mM NaCl, 10 mM MgCl<sub>2</sub>, 5 mM DTT, 5 mM ATP, and 0.001–10 nM reverse gyrase. The beads were observed on an inverted microscope, and images were recorded at 30 Hz. For rapid temperature control, two circulating water baths set at desired temperatures were connected alternately to water channels inside the copper sample holder and copper objective jacket (Fig. 1B). The magnetic beads were pulled upward with a single neodymium magnet (Fig. 1D) or a pair of neodymium magnets (Figs. 1C and 4A). The vertical pulling force *F* was calibrated by tethering the magnetic bead with 16.5- $\mu$ m-long  $\lambda$ -phage DNA and measuring at 23 °C the amplitude of the Brownian fluctuations of the bead. Bead-sinking assays in Fig. 4 were basically as described by Strick et al. (19). We estimated the bead height *z* from the diffraction pattern in the defocused bead image (Fig. S3). ATP hydrolysis was assayed in the same solution as above by monitoring ADP production with reverse phase chromatography. Detailed materials and methods are presented in *SI Methods*.

**ACKNOWLEDGMENTS.** We thank M. Shio and K. Fujino for the stable microscope stage; Ke. Adachi for image analysis programs; members of the K.K. laboratory for technical advice and discussion; and Ku. Adachi, S. Takahashi, K. Sakamaki, and M. Fukatsu for encouragement and laboratory management. This work was supported by Monbukagakusho/Japan Society for the Promotion of Science Kakenhi Grants 16002013, 21000011, and 26221102.

- Kikuchi A, Asai K (1984) Reverse gyrase—A topoisomerase which introduces positive superhelical turns into DNA. *Nature* 309(5970):677–681.
- Suzuki T, et al. (2002) *Sulfolobus tokodaii* sp. nov. (f. *Sulfolobus* sp. strain 7), a new member of the genus *Sulfolobus* isolated from Beppu Hot Springs, Japan. *Extremophiles* 6(1):39–44.
- Forterre P, Mirambeau G, Jaxel C, Nadal M, Duguet M (1985) High positive supercoiling *in vitro* catalyzed by an ATP and polyethylene glycol-stimulated topoisomerase from *Sulfolobus acidocaldarius*. *EMBO J* 4(8):2123–2128.
- Nakasu S, Kikuchi A (1985) Reverse gyrase; ATP-dependent type I topoisomerase from *Sulfolobus*. *EMBO J* 4(10):2705–2710.
- Serre MC, Duguet M (2003) Enzymes that cleave and religate DNA at high temperature: The same story with different actors. *Prog Nucleic Acid Res Mol Biol* 74:37–81.
- Nadal M (2007) Reverse gyrase: An insight into the role of DNA-topoisomerases. *Biochimie* 89(4):447–455.
- Lulchev P, Klostermeier D (2014) Reverse gyrase—Recent advances and current mechanistic understanding of positive DNA supercoiling. *Nucleic Acids Res* 42(13):8200–8213.
- Mirambeau G, Duguet M, Forterre P (1984) ATP-dependent DNA topoisomerase from the archaeobacterium *Sulfolobus acidocaldarius*. Relaxation of supercoiled DNA at high temperature. *J Mol Biol* 179(3):559–563.
- López-García P, Forterre P (1999) Control of DNA topology during thermal stress in hyperthermophilic archaea: DNA topoisomerase levels, activities and induced thermotolerance during heat and cold shock in *Sulfolobus*. *Mol Microbiol* 33(4):766–777.
- Confalonieri F, et al. (1993) Reverse gyrase: A helicase-like domain and a type I topoisomerase in the same polypeptide. *Proc Natl Acad Sci USA* 90(10):4753–4757.
- Déclais AC, Marsault J, Confalonieri F, de La Tour CB, Duguet M (2000) Reverse gyrase, the two domains intimately cooperate to promote positive supercoiling. *J Biol Chem* 275(26):19498–19504.
- Rodríguez AC, Stock D (2002) Crystal structure of reverse gyrase: Insights into the positive supercoiling of DNA. *EMBO J* 21(3):418–426.
- Rudolph MG, del Toro Duany Y, Jungblut SP, Ganguly A, Klostermeier D (2013) Crystal structures of *Thermotoga maritima* reverse gyrase: Inferences for the mechanism of positive DNA supercoiling. *Nucleic Acids Res* 41(2):1058–1070.
- Shibata T, Nakasu S, Yasui K, Kikuchi A (1987) Intrinsic DNA-dependent ATPase activity of reverse gyrase. *J Biol Chem* 262(22):10419–10421.
- Hsieh TS, Capp C (2005) Nucleotide- and stoichiometry-dependent DNA supercoiling by reverse gyrase. *J Biol Chem* 280(21):20467–20475.
- Slesarev AI, Kozyavkin SA (1990) DNA substrate specificity of reverse gyrase from extremely thermophilic archaeobacteria. *J Biomol Struct Dyn* 7(4):935–942.
- Hsieh TS, Plank JL (2006) Reverse gyrase functions as a DNA renaturase: Annealing of complementary single-stranded circles and positive supercoiling of a bubble substrate. *J Biol Chem* 281(9):5640–5647.
- Rodríguez AC (2003) Investigating the role of the latch in the positive supercoiling mechanism of reverse gyrase. *Biochemistry* 42(20):5993–6004.
- Strick TR, Croquette V, Bensimon D (2000) Single-molecule analysis of DNA uncoiling by a type II topoisomerase. *Nature* 404(6780):901–904.
- Dekker NH, et al. (2002) The mechanism of type IA topoisomerases. *Proc Natl Acad Sci USA* 99(19):12126–12131.
- Gore J, et al. (2006) Mechanochemical analysis of DNA gyrase using rotor bead tracking. *Nature* 439(7072):100–104.
- Terekhova K, Gunn KH, Marko JF, Mondragón A (2012) Bacterial topoisomerase I and topoisomerase III relax supercoiled DNA via distinct pathways. *Nucleic Acids Res* 40(20):10432–10440.
- Yogo K, et al. (2012) Direct observation of strand passage by DNA-topoisomerase and its limited processivity. *PLoS ONE* 7(4):e34920.
- Revyakin A, Ebricht RH, Strick TR (2005) Single-molecule DNA nanomanipulation: Improved resolution through use of shorter DNA fragments. *Nat Methods* 2(2):127–138.
- Lipfert J, Wiggin M, Kerssemakers JW, Pedaci F, Dekker NH (2011) Freely orbiting magnetic tweezers to directly monitor changes in the twist of nucleic acids. *Nat Commun* 2:439.
- Duguet M (1993) The helical repeat of DNA at high temperature. *Nucleic Acids Res* 21(3):463–468.
- Jaxel C, et al. (1989) Reverse gyrase binding to DNA alters the double helix structure and produces single-strand cleavage in the absence of ATP. *EMBO J* 8(10):3135–3139.
- Mosconi F, Allemand JF, Bensimon D, Croquette V (2009) Measurement of the torque on a single stretched and twisted DNA using magnetic tweezers. *Phys Rev Lett* 102(7):078301.
- Clauvelin N, Audoly B, Neukirch S (2008) Mechanical response of plectonemic DNA: An analytical solution. *Macromolecules* 41(12):4479–4483.
- Marko JF (2007) Torque and dynamics of linking number relaxation in stretched supercoiled DNA. *Phys Rev E Stat Nonlin Soft Matter Phys* 76(2 Pt 1):021926.
- Plank J, Hsieh TS (2009) Helicase-appended topoisomerases: New insight into the mechanism of directional strand transfer. *J Biol Chem* 284(45):30737–30741.
- Ganguly A, del Toro Duany Y, Klostermeier D (2013) Reverse gyrase transiently unwinds double-stranded DNA in an ATP-dependent reaction. *J Mol Biol* 425(1):32–40.